CARBON letters

Original Articles
Carbon Letters Vol. 20, 19-25 (2016)

NO gas sensing ability of activated carbon fibers modified by an electron beam for improvement in the surface functional group

Mi-Seon Park[1], Sangmin Lee[1], Min-Jung Jung[1], Hyeong Gi Kim[2,*,♣] and Young-Seak Lee[1,*,♣]

[1]Department of Chemical Engineering and Applied Chemistry, Chungnam National University, Daejeon 34134, Korea
[2]Korea Fire Safety Association (KFSA), Daejeon, 34426, Korea

Article Info

Received 12 April 2016
Accepted 5 July 2016

♣Corresponding Author
E-mail: 3son@kfsa.or.kr
youngslee@cnu.ac.kr
Tel: +82-42-638-4119
+82-42-821-7007
*The authors have contributed equally in discussions of the work, performing the experiments, and writing the paper.

Open Access

DOI: http://dx.doi.org/10.5714/CL.2016.20.019

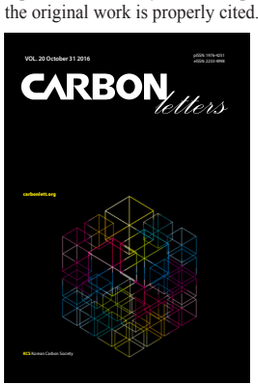

http://carbonlett.org

pISSN: 1976-4251
eISSN: 2233-4998

Abstract

Activated carbon fiber (ACF) surfaces are modified using an electron beam under different aqueous solutions to improve the NO gas sensitivity of a gas sensor based on ACFs. The oxygen functional group on the ACF surface is changed, resulting in an increase of the number of non-carbonyl (-C-O-C-) groups from 32.5% for pristine ACFs to 39.53% and 41.75% for ACFs treated with hydrogen peroxide and potassium hydroxide solutions, respectively. We discover that the NO gas sensitivity of the gas sensor fabricated using the modified ACFs as an electrode material is increased, although the specific surface area of the ACFs is decreased because of the recovery of their crystal structure. This is attributed to the static electric interaction between NO gas and the non-carbonyl groups introduced onto the ACF surfaces.

Key words: activated carbon, adsorption, functional groups, gas sensor

1. Introduction

Nitrogen oxide (NO_x) is produced in various chemical production processes, metal plating processes, and internal combustion engines that operate on fossil fuels. In high concentrations, the gas stimulates the respiratory organ, which can induce coughing, pharyngalgia, dizziness, headaches, etc. Nitric oxide (NO) is the main gas that leads to the production of nitrogen oxide contaminants in the atmosphere. Therefore, the detection of NO gas in the atmosphere is important [1,2].

When used as electrode materials for gas sensors, carbon materials such as carbon nanotubes, graphene oxides, and activated carbon fibers (ACFs) have shown superior gas sensing ability at room temperature, whereas metal oxides can only be operated at high temperature (i.e., above 300°C) [3,4]. Among these carbon materials, ACFs exhibit high sensitivity because of the presence of micropores, which can rapidly adsorb angstrom-sized gas molecules. In addition, a large amount of carbon materials can be placed on small-sized electrodes because of their lower density compared to that of metals. Finally, they are chemically resistant in various environments at room temperature.

The interaction between gas molecules and functional groups has also been actively studied as a key factor in the detection of gases. Various surface treatments to introduce specific functional groups onto electrode materials have been investigated. In the case of carbon materials, the developed surface treatments include acid/base, ozone, electrical, and fluorination treatments [5-8]. However, these treatments are time-consuming and require additional supporting equipment.

Electron beam (E-beam) irradiation has been rapidly developed as a polymer processing technique [9,10]. It is used for polymer modification, such as cross-linking, curing, and grafting, on the basis of the optical transparency of the system and because chemical/photo-

chemical initiator is not required [11]. E-beam-triggered polymerization occurs rapidly and is accompanied by the generation of free-radicals, similar to other polymerization methods. The molecular weight of the resulting polymer rapidly increases when free-radical termination is minimized [12].

In this study, the functional groups on the ACFs were modified by E-beam irradiation under aqueous solutions. The structural, textural, and chemical properties of the ACFs modified by E-beam irradiation were investigated. In addition, the electrochemical properties of the electrode material of the NO gas sensor were also evaluated. The results demonstrate that the E-beam irradiation can modify carbon material surfaces in an aqueous solution, and that the modified materials exhibit improved sensitivity to NO gas when used as gas sensor electrode materials.

2. Experimental

2.1. Materials

The pitch-based ACF (product name: A7) used in this study was obtained from Osaka Gas Co., Ltd., Japan. The chemicals used to modify the ACF surfaces were hydrogen peroxide solution (H_2O_2, 34.5%) and potassium hydroxide solution (KOH, 4 M), which were purchased from SAMCHUN Chemical, Co., Ltd., Pyeongtaek, Korea. *N*,*N*-Dimethylformamide (DMF) was used as a dispersion agent for gas-sensor electrode materials.

2.2. ACF surface modification by E-beam irradiation

Samples of the ACFs (1 g) were immersed deeply in 50 mL of H_2O_2 or KOH solution, for 15 h. These chemicals were used as solutions representing an acid and a base, respectively. The ACFs were transferred to tempered glass schales after sufficient wetting with the chemicals. The schales containing the ACFs were covered with a transparent lid and placed on a conveyor passing under the E-beam accelerator. The transport speed of the conveyor was 4 m/min. The E-beam accelerator generated an electron energy of 1.14 MeV under an accelerating current of 15.7 mA. In addition, the absorbed dose was controlled to 50 kGy per turn; the total absorbed dose was 100 kGy. The E-beam irradiation was performed at room temperature. The sample was named according to the chemical solution used and the E-beam absorbed dose. Pristine ACFs were referred to as A7. The ACFs irradiated with the E-beam under hydrogen peroxide solution were referred to as A7-H100. The ACFs irradiated with the E-beam under KOH solution were referred to as A7-K100. All of the prepared samples were used as electrode materials in a gas sensor.

2.3. Fabrication of the gas sensor

The prepared samples (0.01 g) were dispersed in DMF (1 g) and then sonicated for 10 min to uniformly disperse the samples in the DMF. The dispersion solution (5 μL) was dropped onto an Si wafer, which was oxidized and sputtered with Pt, using a micro-pipette (Transferpette® electronic pipette; BrandTech Scientific Inc., Essex, CT, USA) and then dried at room temperature for 3 h. Finally, a silver wire (Φ 0.1) was connected to the Pt electrode containing the samples using silver paste (Elcoat P-100, 10^{-4} Ω cm Cans, Korea). The Si-wafer oxidation conditions were as follows: a Si-wafer was sonicated and washed sequentially with acetone, ethanol, and water for 30 min. The pre-treated Si-wafer was heated at 900°C for 2 h under a nitrogen atmosphere to be covered with a SiO_2 film. The Pt sputtering conditions are as follows: prior to the Pt sputtering, Ti was sputtered onto the SiO_2/Si wafer to prevent the Pt electrode from peeling forward. The SiO_2/Si wafer was placed in a sputter-coater (DC magnetic sputtering; Hanbaek vacuum, Bucheon, Korea) chamber, which was subsequently evacuated to 3.5×10^{-3} Pa. The target power was 250 mA and 415 V and the Ti sputtering was conducted for 20 s. After the Ti sputtering, Pt sputtering was performed at 20 mA and 485 V for 200 s under the same vacuum conditions as used for Ti sputtering [13].

2.4. Characteristics

Structural changes in the ACFs after the E-beam irradiation were investigated using Raman spectroscopy (LabRam high resolution; Horiba Jobin-Yvon, Villeneuve-d'Ascq, France). The energy source was an Ar-ion laser (514.532 nm). Crystal structures of the samples were determined using X-ray diffraction (XRD; D8 DISCOVER, Bruker AXS, Karlsruhe, Germany). The XRD analyses were conducted in the range of 5°–60° using a Cu target. The textural characteristics of the prepared sample were assessed through N_2 adsorption at 77 K with a BELSORP-max surface area and porosimetry system (BEL Inc., Japan). Each sample was degassed at 150°C for 6 h before analysis. The specific surface areas and pore structure of the prepared ACFs were evaluated using the Brunauer-Emmett-Teller (BET) method. The pore size distribution was calculated by the Horvath-Kawazoe (HK) method from the nitrogen adsorption isotherm curves. The changes in the surface functional groups of the prepared ACFs were investigated using X-ray photoelectron spectroscopy (XPS; MultiLab 2000 spectrometer, Thermo Electron Corp., England); the instrument was equipped with an Al K α (1485.6 eV) X-ray source that was operated at an anode voltage of 14.9 keV, a filament current of 4.6 A, and an emission current of 20 mA.

2.5. Evaluation of gas sensing ability

The prepared ACFs were evaluated as electrode materials for gas sensors. The gas sensing tests were performed using a programmable electrometer (Keithley 6514), which provides an electrical resistance according to the reaction between electrode materials and gas molecules. This measurement was conducted in a stainless steel chamber with a volume of 1500 cm^3. The chamber was connected to separate gas cylinders containing NO and N_2. The prepared gas sensor was placed in a sealed chamber. Initially, N_2 gas was flowed into the chamber to stabilize the electrical resistance of the gas sensor; 1000 ppm NO gas was then flowed into the chamber. The N_2 gas was used as the carrier gas for further control of the gas concentrations. A mixture of the two gases was then prepared with 100 ppm NO in the chamber. The total flow rate of the gases was 500 sccm, which was fixed in all cases.

DOI: http://dx.doi.org/10.5714/CL.2016.20.019

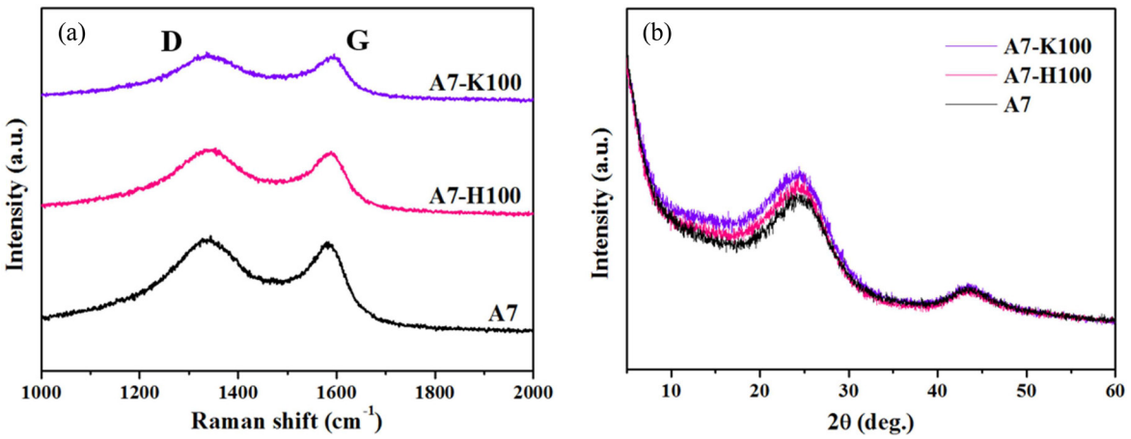

Fig. 1. (a) Raman spectra and (b) X-ray diffraction patterns of the pristine activated carbon fibers (ACFs) and electron beam-irradiated ACFs.

The gas sensing tests were conducted at room temperature. To ensure accurate observation, the NO gas was injected into the chamber for 10 min after the electrical resistance was allowed to stabilize for 30 min.

3. Results and Discussion

3.1. Structural properties

The structural properties of the ACFs irradiated with the E-beam in hydrogen peroxide and potassium solutions were investigated by Raman analysis. Raman analysis is a valuable tool to characterize the electronic structure of carbon materials; it is particularly useful for determining ordered and disordered crystal structures in graphene layers [14-16]. The Raman spectra of ACFs generally show two prominent D and G bands. The G band originates from an in-phase vibration of the E_{2g} mode of the sp^2 carbon domains, whereas the D band is induced by the disordered crystal structure with symmetry breaking or edges of graphene [15,17]. The Raman spectra of the modified ACFs are shown in Fig. 1a. All the G bands of the E-beam-irradiated ACFs were red-shifted from 1584 cm^{-1}, indicating that the sp^2 domains were repaired by E-beam irradiation [18]. In addition, the intensity of the D band was substantially decreased. These two effects resulted in a decrease of the relative intensity ratio between the D and G bands (I_D/I_G), as shown in Table 1. The I_D/I_G decreased from 1.14 for A7 to 1.09 and 1.08 for A7-H100 and A7-K100, respectively. The magnitude of the decreases was similar in the two solutions, indicating that the structural properties of ACFs could be changed by E-beam irradiation irrespective of the solution type. The restoration of the sp^2 domains by E-beam irradiation suggests a decrease in the number of edges, which act as pores in the ACFs. XRD patterns in Fig. 1b supported the recovery of crystallinity, showing an increase of peak intensity at approximately 26°, which indicates the (0 0 2) crystal plane of carbon materials. Another carbon material peak at 43° was not changed by E-beam irradiation. Therefore, we examined the pore structures of the E-beam-irradiated ACFs, as described in the next section.

Table 1. The ratio of I_D/I_G of pristine ACFs and electron beam-irradiated ACFs

Sample	A7	A7-H100	A7-K100
I_D/I_G	1.14	1.09	1.08

I_D/I_G, intensity ratio between the D and G bands; ACFs, activated carbon fibers.

3.2. Textural properties

The pore structure of the ACFs treated with the E-beam and chemically was investigated by a N_2 adsorption-desorption analysis at 77 K. The isotherm curves of the modified ACFs are shown in Fig. 2a. All the samples exhibited a sharp increase in the quantity adsorbed below 0.01 P/P_0, with no further increase of the quantity adsorbed above 0.01 P/P_0. Therefore, all adsorption isotherm curves are classified as type I according to the International Union of Pure and Applied Chemistry (IUPAC) classification and indicate the existence of micropores in the samples [19]. As shown in Table 2, the BET specific surface area (S_{BET}) and total pore volume (V_t) of the modified ACFs dramatically decreased in both solutions. The S_{BET} of A7 was determined to be 659 $m^2\ g^{-1}$ with a V_t of 0.263 mL g^{-1}; by contrast the S_{BET} and V_t of the ACFs irradiated with the E-beam in hydrogen peroxide solution were 460 $m^2\ g^{-1}$ and 0.191 mL g^{-1} and those of the ACFs irradiated in potassium hydroxide solution were 480 $m^2\ g^{-1}$ and 0.197 mL g^{-1}, respectively. The pore size distribution curves of the treated ACFs were calculated by the HK method from the adsorption branch, as shown in Fig. 2b. The results indicated that the E-beam irradiation of ACFs in the solution collapsed the micropores, although the pore size of the ACFs slightly increased from 6.1 Å to 6.4–6.7 Å. E-beam irradiation in aqueous solutions is known to generate various ions and molecules, including ·OH, ·H, e^-_{aq}, H_2, H_2O_2, and H_3O^+ because of the radiolysis of water. Among these species, hydrated electrons (e^-_{aq}) can reduce the specific target [20]. The hydrogen peroxide solution includes more possible hydrated electrons

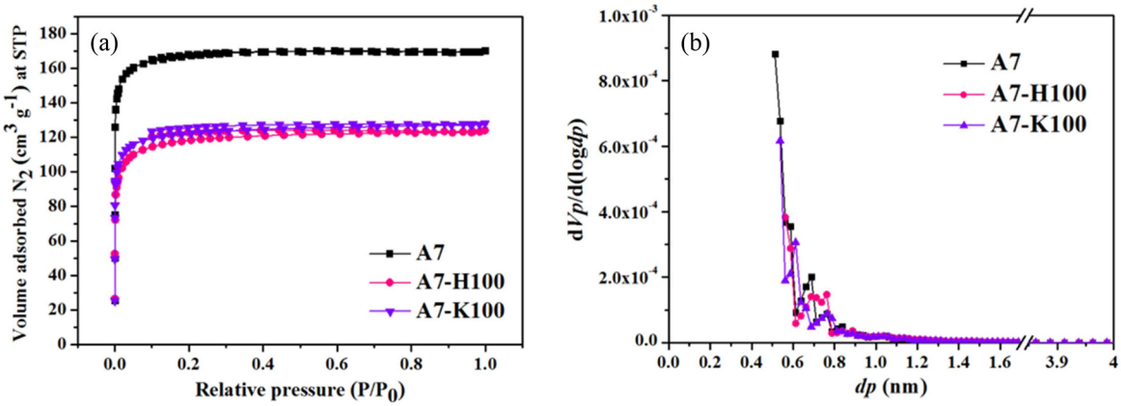

Fig. 2. (a) N_2 adsorption-desorption isotherms and (b) Horvath-Kawazoe (HK) pore size distributions of the pristine activated carbon fibers (ACFs) and electron beam-irradiated ACFs.

Table 2. BET specific surface area and porous parameters of the ACFs

Sample	S_{BET}[a] (m^2 g^{-1})	V_t[b] (mL g^{-1})	V_{micro}[c] (mL g^{-1})	V_{meso}[d] (mL g^{-1})	D_{micro}[e] (Å)
A7	659	0.263	0.262	0.001	6.1
A7-H100	460	0.191	0.189	0.002	6.7
A7-K100	480	0.197	0.195	0.002	6.4

BET, Brunauer-Emmett-Teller; ACFs, activated carbon fibers.
[a]BET specific surface area calculated from the linear part of the BET plot.
[b]The total pore volume was taken from the volume of nitrogen adsorbed at about $P/P_0 = 0.99$.
[c]The micropore volume was estimated by the t-plot.
[d]$V_t - V_{micro}$.
[e]The average micropore diameter was estimated by the t-plot method.

compared to the potassium hydroxide solution. Therefore, the crystal structure of the E-beam-irradiated ACFs in hydrogen peroxide solution (A7-H100) was reduced to a greater extent, which is consistent with the aforementioned Raman analysis results, resulting in a greater decrease of the S_{BET} compared to that in the case of A7-K100.

3.3. Effects of E-beam on the chemical composition of ACFs in different solutions

An XPS elemental analysis was performed to examine changes in the chemical composition of the ACFs. The XPS spectra of the modified ACFs over a wide binding energy range of approximately ~100–700 eV are shown in Fig. 3a. The peaks at 284.5 eV and 532.8 eV correspond to the C1s and O1s signals, respectively [21]. The O1s peak increased in intensity after E-beam irradiation in an aqueous solution, as shown in Table 3. This demonstrates that E-beam irradiation can be used as a new treatment for carbon material surfaces. The fitting of the O1s peak was resolved into four components centered at 531.2, 532.4, 533.5, and 534.7 eV (several pseudo-Voigt functions [sums of the Gaussian and Lorentzian functions]) using a peak analysis program (Unipress Co., Tampa, FL, USA). The pseudo-Voigt function is given by the following eq 1 [22]:

Table 3. Elemental analysis (XPS) of the pristine ACFs and electron beam-irradiated ACFs

Sample	A7	A7-H100	A7-K100
C (at%)	88.33	86.26	83.58
O (at%)	11.67	13.74	16.42
O/C (%)	13.21	15.92	19.64

XPS, X-ray photoelectron spectroscopy; ACFs, activated carbon fibers.

$$F(E) = H\left[(1-S)\exp\left(\left(-\ln(2)\left(\frac{E-E_0}{FWHM}\right)^2\right) + \frac{S}{1+\left(\frac{E-E_0}{FWHM}\right)^2}\right)\right] \quad (1)$$

where $F(E)$ is the intensity at energy E, H is the peak height, E_0 is the peak center, FWHM is the full-width at half-maximum, and S is a shape function related to both the symmetry and Gaussian-Lorentzian mixing ratio. The results of the deconvolution are shown in Fig. 3b-d and listed in Table 4. These peaks represent the quinone, phenolic, non-carbonyl, and carboxyl group for O(1) –(4), respectively [23,24]. Among them, the phenolic and carboxyl groups are only active as anionic species in an environment of adequate basicity, mainly at the basal plane [25]. The quinone group shows strong electrochemical properties in the presence of meso-

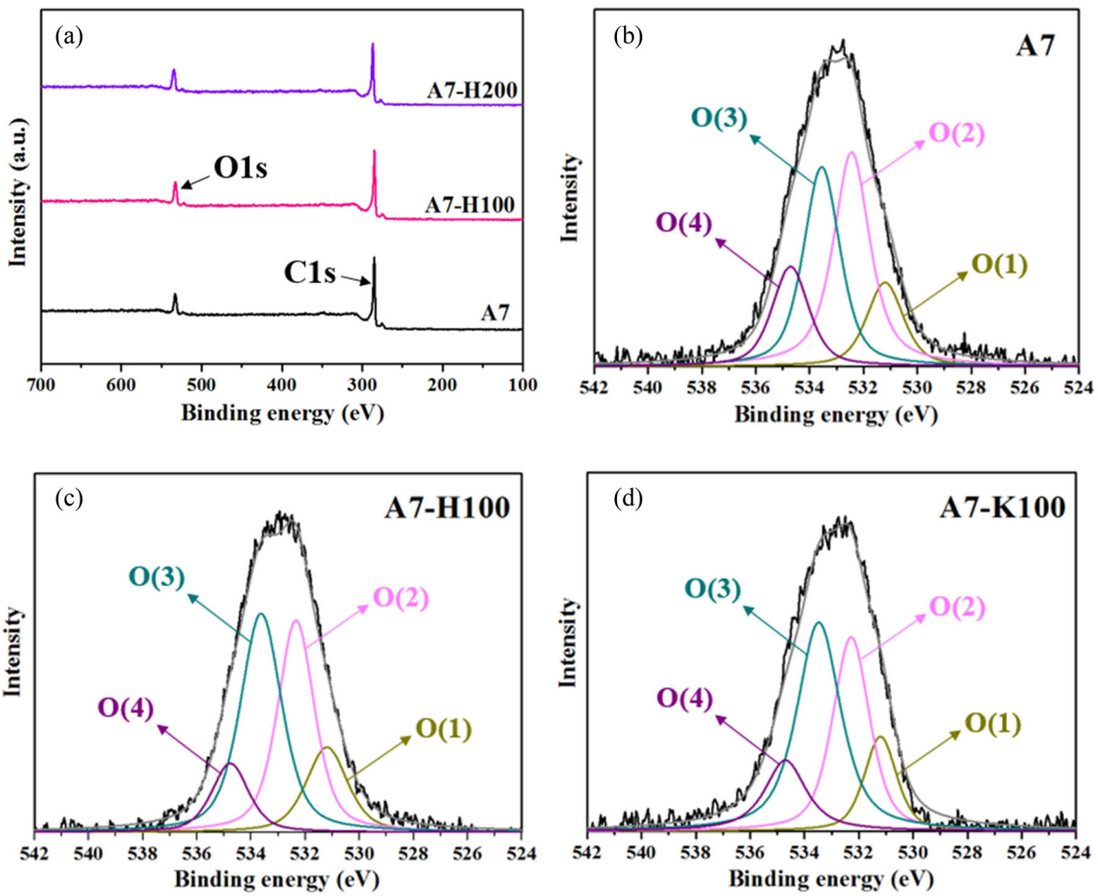

Fig. 3. (a) X-ray photoelectron spectroscopy (XPS) spectra of the pristine activated carbon fibers (ACFs) and electron beam-irradiated ACFs. Deconvoluted XPS O1s spectra of (b) A7, (c) A7-H100, and (d) A7-K100.

Table 4. Assignment and peak parameters for O1s component of the pristine ACFs and electron beam-irradiated ACFs

Component	Assignment	Binding energy (eV)	Concentration (%)		
			A7	A7-H100	A7-K100
O(1)	O=C	531.2	13.66	15.37	13.19
O(2)	HO-C	532.4	37.59	34.03	30.90
O(3)	-C-O-C-	533.5	32.50	39.53	41.75
O(4)	-COOH	534.7	16.25	11.07	14.16

ACFs, activated carbon fibers.

pores [26]. The number of non-carbonyl (-C-O-C-) groups in lactone was meaningfully changed on the ACF surfaces. In addition, for A7-K100, the concentration of -C-O-C- group only increased in contrast with decreases in the other oxygen group concentrations, as shown in Table 4. It can be considered that potassium cations (K^+) that were generated after E-beam irradiation can react with oxygen functional groups, such as O=C, HO-C, and HOOC-. They then changed into -C-O-C- groups on the carbon surfaces. These differences in the chemical composition of the modified ACFs were expected to affect the electrochemical properties of the corresponding ACF-based gas sensor, as discussed in section 3.4.

3.4. NO gas sensing

The electrochemical properties of the modified ACFs, which exhibit differences in their surface oxygen functional groups, were estimated on the basis of their performance as electrode materials in gas sensors used to detect NO gas. The sensitivity of the gas sensors was calculated using the follow-

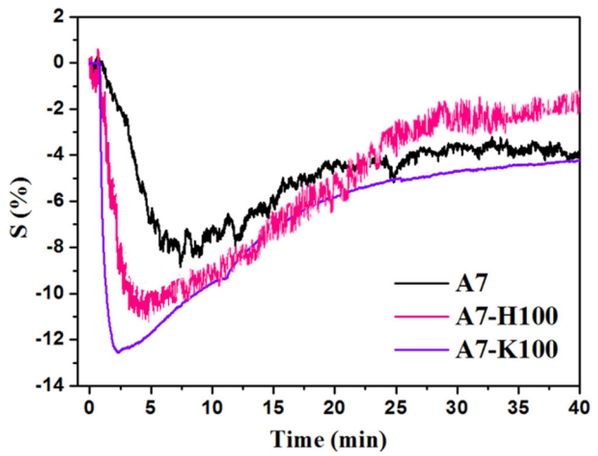

Fig. 4. NO gas sensing results of the pristine activated carbon fibers (ACFs) and electron beam-irradiated ACFs.

ing equation [1,27]:

$$S(\%) = \frac{\Delta R}{R_{N_2}} \times 100 = \frac{R_{NO} - R_{N_2}}{R_{N_2}} \times 100 \quad (2)$$

where R_{N_2} and R_{NO} are the resistance values measured upon exposure to N_2 gas and NO gas, respectively. The gas sensing results are shown in Fig. 4. NO gas was injected at 0 min to the prepared gas sensor in the chamber. The NO gas flow was then stopped after 10 min. All of the prepared gas sensors showed a decrease in resistance in the presence of NO gas because carbon materials are p-type semiconductors with hole carriers, and NO gas is an oxidizing gas that transports electrons from other materials [13]. A gas sensor based on the A7 sample exhibited approximately 8% sensitivity for NO gas. In general, the sensitivity of the gas sensors based on carbon materials depends on $S_{BET,}$ particularly micropores [28]. However, the A7-H100 and A7-K100 based gas sensors displayed higher sensitivities of approximately 11% and 12%, respectively, although they had lower S_{BET} values. These results are consistent with the changes in the oxygen functional groups and non-carbonyl (-C-O-C-) groups. The non-carbonyl groups can more positively charge the carbon material through interactions between the -C-O-C- groups and NO gas, as shown in Fig. 5. An increase of hole carriers reduces the resistance, which induces an increase in NO gas sensitivity.

4. Conclusions

ACFs were treated with an E-beam under different aqueous solutions. The E-beam irradiation modified the structural properties of the ACFs, which exhibited a decrease in I_D/I_G values from 1.14 for the raw ACFs to 1.09 and 1.08 for ACFs treated with hydrogen peroxide and potassium hydroxide solutions, respectively. This change contributed to the generation of hydrated electrons according to the radiolysis of the used chemicals. The improvement in crystallinity led to a decrease of the specific surface area of ACFs. However, the NO gas sensitivity of the gas sensor fabricated using E-beam-irradiated ACFs increased to 11%–12%. This increase in sensitivity was induced by the change in the oxygen functional groups of the ACF surfaces under E-beam irradiation in an aqueous solution. In particular, the non-carbonyl (-C-O-C-) groups interacted with NO gas and increased the number of hole carriers, which enhanced the NO gas sensitivity of the ACFs-based gas sensor.

Conflict of Interest

No potential conflict of interest relevant to this article was reported.

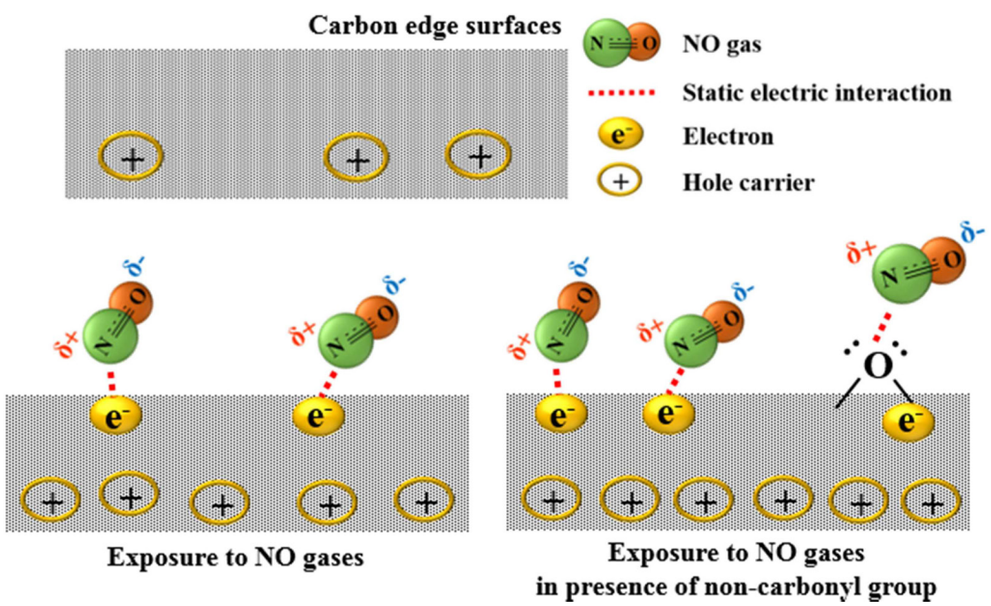

Fig. 5. Schematic representation of the non-carbonyl group effect on carbon material surfaces.

Acknowledgements

This research was supported by a grant from the National Research Foundation of Korea (NRF) funded by the Ministry of Science, ICT & Future Planning (No. 2013M2A2A6043697).

References

[1] Kang SC, Im JS, Lee SH, Bae TS, Lee YS. High-sensitivity gas sensor using electrically conductive and porosity-developed carbon nanofiber. Colloids Surf A Physicochem Eng Asp, **384**, 297 (2011). http://dx.doi.org/10.1016/j.colsurfa.2011.04.001.

[2] Kukkola J, Mäklin J, Halonen N, Kyllönen T, Tóth G, Szabó M, Shchukarev A, Mikkola JP, Jantunen H, Kordás K. Gas sensors based on anodic tungsten oxide. Sens Actuator B Chem, **153**, 293 (2011). http://dx.doi.org/10.1016/j.snb.2010.10.043.

[3] Zhang J, Hu J, Zhu ZQ, Gong H, O'Shea SJ. Quartz crystal microbalance coated with sol–gel-derived indium–tin oxide thin films as gas sensor for NO detection. Colloids Surf A Physicochem Eng Asp, **236**, 23 (2004). http://dx.doi.org/10.1016/j.colsurfa.2004.01.010.

[4] Jung JY, Lee CS. Characteristics of the TiO_2/SnO_2 thick film semiconductor gas sensor to determine fish freshness. J Ind Eng Chem, **17**, 237 (2011). http://dx.doi.org/10.1016/j.jiec.2011.02.012.

[5] Peng H, Li Y, Jiang C, Luo C, Qi R, Huang R, Duan CG, Travas-Sejdic J. Tuning the properties of luminescent nitrogen-doped carbon dots by reaction precursors. Carbon, **100**, 386 (2016). http://dx.doi.org/10.1016/j.carbon.2016.01.029.

[6] Krawczyk P. Properties of an EG/Fe/C composite modified by ozone treatment. Carbon, **65**, 374 (2013). http://dx.doi.org/10.1016/j.carbon.2013.08.022.

[7] Park MS, Lee YS. Functionalization of graphene oxide by fluorination and its characteristics. J Fluor Chem, **182**, 91 (2016). http://dx.doi.org/10.1016/j.jfluchem.2015.12.011.

[8] Park MS, Kim KH, Lee YS. Fluorination of single-walled carbon nanotube: the effects of fluorine on structural and electrical properties. J Ind Eng Chem, **37**, 22 (2016). http://dx.doi.org/10.1016/j.jiec.2016.03.024.

[9] Park MS, Ko Y, Jung MJ, Lee YS. Stabilization of pitch-based carbon fibers accompanying electron beam irradiation and their mechanical properties. Carbon Lett, **16**, 121 (2015). http://dx.doi.org/10.5714/cl.2015.16.2.121.

[10] Jung JY, Park MS, Kim MI, Lee YS. Novel reforming of pyrolized fuel oil by electron beam radiation for pitch production. Carbon Lett, **15**, 262 (2014). http://dx.doi.org/10.5714/cl.2014.15.4.262.

[11] Vautard F, Ozcan S, Poland L, Nardin M, Meyer H. Influence of thermal history on the mechanical properties of carbon fiber–acrylate composites cured by electron beam and thermal processes. Compos Part A Appl Sci Manuf, **45**, 162 (2013). http://dx.doi.org/10.1016/j.compositesa.2012.08.025.

[12] Schlemmer B, Bandari R, Rosenkranz L, Buchmeiser MR. Electron beam triggered, free radical polymerization-derived monolithic capillary columns for high-performance liquid chromatography. J Chromatogr A, **1216**, 2664 (2009). http://dx.doi.org/10.1016/j.chroma.2008.09.003.

[13] Park MS, Kim KH, Kim MJ, Lee YS. NH_3 gas sensing properties of a gas sensor based on fluorinated graphene oxide. Colloids Surf A Physicochem Eng Asp, **490**, 104 (2016). http://dx.doi.org/10.1016/j.colsurfa.2015.11.028.

[14] Ferrari AC, Meyer JC, Scardaci V, Casiraghi C, Lazzeri M, Mauri F, Piscanec S, Jiang D, Novoselov KS, Roth S, Geim AK. Raman spectrum of graphene and graphene layers. Phys Rev Lett, **97**, 187401 (2006). http://dx.doi.org/10.1103/physrevlett.97.187401.

[15] Ferrari AC. Raman spectroscopy of graphene and graphite: disorder, electron–phonon coupling, doping and nonadiabatic effects. Solid State Commun, **143**, 47 (2007). http://dx.doi.org/10.1016/j.ssc.2007.03.052.

[16] Mowry M, Palaniuk D, Luhrs CC, Osswald S. In situ Raman spectroscopy and thermal analysis of the formation of nitrogen-doped graphene from urea and graphite oxide. RSC Adv, **3**, 21763 (2013). http://dx.doi.org/10.1039/c3ra42725k.

[17] Krishnamoorthy K, Kim SJ. Mechanochemical preparation of graphene nanosheets and their supercapacitor applications. J Ind Eng Chem, **32**, 39 (2015). http://dx.doi.org/10.1016/j.jiec.2015.09.012.

[18] Kang M, Lee DH, Yang J, Kang YM, Jung H. Simultaneous reduction and nitrogen doping of graphite oxide by using electron beam irradiation. RSC Adv, **5**, 104502 (2015). http://dx.doi.org/10.1039/c5ra20199c.

[19] Gregg SJ, Sing KSW. Adsorption Surface Area and Porosity, 2nd ed., Academy Press, London (1982).

[20] Kang M, Lee DH, Kang YM, Jung H. Electron beam irradiation dose dependent physico-chemical and electrochemical properties of reduced graphene oxide for supercapacitor. Electrochim Acta, **184**, 427 (2015). http://dx.doi.org/10.1016/j.electacta.2015.10.053.

[21] Guo HL, Su P, Kang X, Ning SK. Synthesis and characterization of nitrogen-doped graphene hydrogels by hydrothermal route with urea as reducing-doping agents. J Mater Chem A, **1**, 2248 (2013). http://dx.doi.org/10.1039/c2ta00887d.

[22] Kim JG, Im JS, Bae TS, Kim JH, Lee YS. The electrochemical behavior of an enzyme biosensor electrode using an oxyfluorinated pitch-based carbon. J Ind Eng Chem, **19**, 94 (2013). http://dx.doi.org/10.1016/j.jiec.2012.07.008.

[23] Zhang C, Duan Y, Xing B, Zhan L, Qiao W, Ling L. Influence of nitrogen hetero-substitution on the electrochemical performance of coal-based activated carbons measured in non-aqueous electrolyte. Min Sci Technol, **19**, 295 (2009). http://dx.doi.org/10.1016/s1674-5264(09)60055-7.

[24] Velo-Gala I, Lo´pez-Peñalver JJ, Sánchez-Polo M, Rivera-Utrilla J. Surface modifications of activated carbon by gamma irradiation. Carbon, **67**, 236 (2014). http://dx.doi.org/10.1016/j.carbon.2013.09.087.

[25] DeRuiter J. Carboxylic Acids Part 2, Principles of Drug Action 1, Spring 2005 (2005).

[26] Yu HR, Cho S, Jung MJ, Lee YS. Electrochemical and structural characteristics of activated carbon-based electrodes modified via phosphoric acid. Microporous Mesoporous Mater, **172**, 131 (2013). http://dx.doi.org/10.1016/j.micromeso.2013.01.018.

[27] Im JS, Kang SC, Lee SH, Lee YS. Improved gas sensing of electrospun carbon fibers based on pore structure, conductivity and surface modification. Carbon, **48**, 2573 (2010). http://dx.doi.org/10.1016/j.carbon.2010.03.045.

[28] Kang SC, Im JS, Lee YS. Improved sensitivity of an NO gas sensor by chemical activation of electrospun carbon fibers. Carbon Lett, **12**, 21 (2011). http://dx.doi.org/10.5714/cl.2011.12.1.021.